Eclética Química

Original article

revista.iq.unesp.br

| Vol. 48 | n. 2 | 2023 |

Synthesis, structural and spectroscopic properties of Co(II), Ni(II) and Cu(II) complexes with 2-((2-chlorobenzylidene)amino) acetohydrazide hydrate and their Antimicrobial and antioxidant activities

Fathi Mohammed Al-Azab[1], Yasmin Mosa'd Jamil[1+], Amani Ahmed Al-Gaadbi[1]

1. Sana'a University, Faculty of Science, Sana'a, Yemen.

+Corresponding author: Yasmin Mos'ad Jamil, **Phone:** +967-771952842, **Email address:** y.jamil@su.edu

ARTICLE INFO

Article history:
Received: November 14, 2022
Accepted: February 24, 2023
Published: April 01, 2023

Section Editors: Rogéria Rocha Gonçalves

Keywords:
1. Schiff base
2. powder X-ray diffraction
3. antioxidant activity

ABSTRACT: The current study was purposed to prepare Co(II), Ni(II) and Cu(II) complexes with the ligands derived from 2-chlorobenzaldehyde, glycine and hydrazine hydrate. The obtained compounds were characterized by different physicochemical studies such as elemental analysis, atomic absorption, molar ratio analysis, electronic absorption (UV-Vis spectroscopy), magnetic properties, FTIR spectroscopy, ^{1}H–NMR, ^{13}C-NMR, conductance measurements and XRD. Antimicrobial and antioxidant activities were also calculated. The antibacterial activity was evaluated by the diffusion method against two Gram-positive and two Gram-negative bacteria, while antifungal activity was assessed against two fungal strains by using the agar method. The ligand with Schiff base and hydrazide groups and its complexes showed better biological activity. The results showed that the most metal complexes have much higher antibacterial and antifungal activity compared to the parent ligand. The antioxidant activity of 3.7453 mg of the ligand exhibited excellent activity as the activity of 1 mg of ascorbic acid which is used as a standard antioxidant.

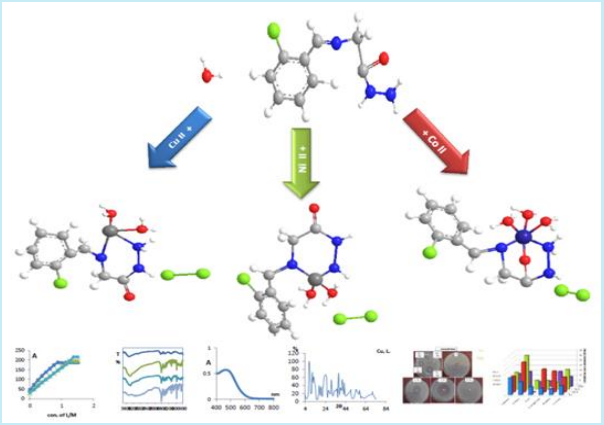

Eclética Química, vol. 48, n. 2, 2023, 66-82
ISSN: 1678-4618
DOI: 10.26850/1678-4618eqj.v48.2.2023.p66-82

1. Introduction

1.1 Schiff bases and hydrazides

Schiff bases are usually prepared by the condensation of a carbonyl compound with a primary amine (Malakyan *et al*., 2016). Imine or azomethine groups are present in various natural, natural-derived and nonnatural compounds (Safoura, 2014). They are used in many fields such as biological activities, analytical chemistry, corrosion inhibitors, fungicidal, agrochemical, electrical conductivity, magnetism, ion exchange, nonlinear optics, catalysis (Emriye, 2016), crystal engineering (Al Zoubi, 2013), and medical substrates (Savalia *et al*., 2013). Hydrazides include C(=O)NHNH$_2$ group, and were produced as far back as 1895 by Kurzius (Majumdar *et al*., 2014). Hydrazides have been used widely in medicine, catalysis, and analytical chemistry (Salawu *et al*., 2018), and are highly useful starting materials and intermediates in the synthesis of heterocyclic intermediates in the synthesis of heterocyclic molecules. They have been investigated due to their antitumor and biocidal activity, also they have been used widely as antituberculosis compounds because of their ability to form metal chelates (Mathew *et al*., 2006). A large number of different Schiff base ligands have been used for excellent selectivity, sensitivity, and stability for specific metal ions such as Ag(II) Al(III), Co(II), Cu(II), Gd(III), Hg(II), Ni(II), Pb(II), Y(III), and Zn(II) (Ashraf *et al*., 2011).

The aim of the present work is to synthesize new compounds containing derivatives of ligands via Schiff base with hydrazide which is derived from 2-chlorobenzaldehyde, glycine and hydrazine hydrate which reacted with Co, Ni and Cu ions to form new complexes.

2. Experimental

2.1 Reagents and solutions

All chemicals used are commercially available from BDH.

2.2 Instrumentation

The melting points were determined in glass capillary tubes in degrees Celsius. Molar conductance in dimethyl sulfoxide (DMSO) (10^{-3} mol L^{-1} solution at 25 °C) and molar ratio were measured on Jenway conductivity meter model 4510. The ligand and its complexes were characterized by comparison of spectroscopic data, infrared (IR) spectra of the ligand and metal complexes were measured using FT/IR – 140, Jasco, Japan in KBr pellets. ^{1}H and ^{13}C nuclear magnetic resonance (NMR) spectra were recorded in a Varian FT – 300 MHz spectrometer in d_6-DMSO solvent using tetramethylsilane as internal standard. Ultraviolet-visible (UV-Vis) spectra and antioxidant activity measurements (by ferric-bipyridine method) (Specord 200, Analytilk Jena, Germany) using DMSO and methanol as the reference and solvent, respectively. The magnetic susceptibilities of the complexes were measured at room temperature using Gouy's method by a magnetic susceptibility balance from Johnson Metthey and Sherwood model. Carbon, hydrogen, and nitrogen were estimated by Vario ELFab. Nr. 11042023. The X-ray powder diffraction patterns of the ligand and the solid complexes were obtained using XD-2 (Shimadzu ED-720), X-ray powder diffractometer at a voltage of 35 KV and current of 20 mA using CuKα radiation generator in the range $5° < 2\theta < 70°$ with a 1 min^{-1} scanning rate and a wavelength of 0.154056 nm. Microbiological analysis was carried out using the filter paper disc method.

2.3 Synthesis of Schiff base hydrazide ((2-chlorobenzylidene)amino)acetohydrazide hydrate = L

The solid ligand was prepared in 1:1:1 molar ratio as shown in Fig. 1 by adding dropwise of an ethanolic solution of glycine (0.01 mol) to an ethanolic solution of the aldehyde (0.01 mol) with stirring. The mixture was refluxed for 3 h with constant stirring and heating (Gao, 2013) until light brown solution of the Schiff base is formed. Then, addition of hydrazine hydrate drop by drop with constant stirring to the hot solution of the first part of the Schiff base until light brown precipitate is formed. The resulting precipitate was filtered off and washed with ethanol until the solution become clear then was left to dry.

2.4 Synthesis of the complexes

Generally, all the solid complexes were prepared as shown in Fig. 2 by adding dropwise of an methanolic solution of the hydrated metal chlorides (0.008 mol) to an methanolic solution of the ligand (Schiff base hydrazide 0.008 mol) with stirring. The mixture of each was refluxed for 4 to 6 h with constant stirring until colored precipitates are formed. All the materials solutions were in 1:1 molar ratio. The resulting precipitates were filtered off and washed with methanol even become a clear solution, then left them to dry.

Eclética Química, vol. 48, n. 2, 2023, 66-82
ISSN: 1678-4618
DOI: 10.26850/1678-4618eqj.v48.2.2023.p66-82

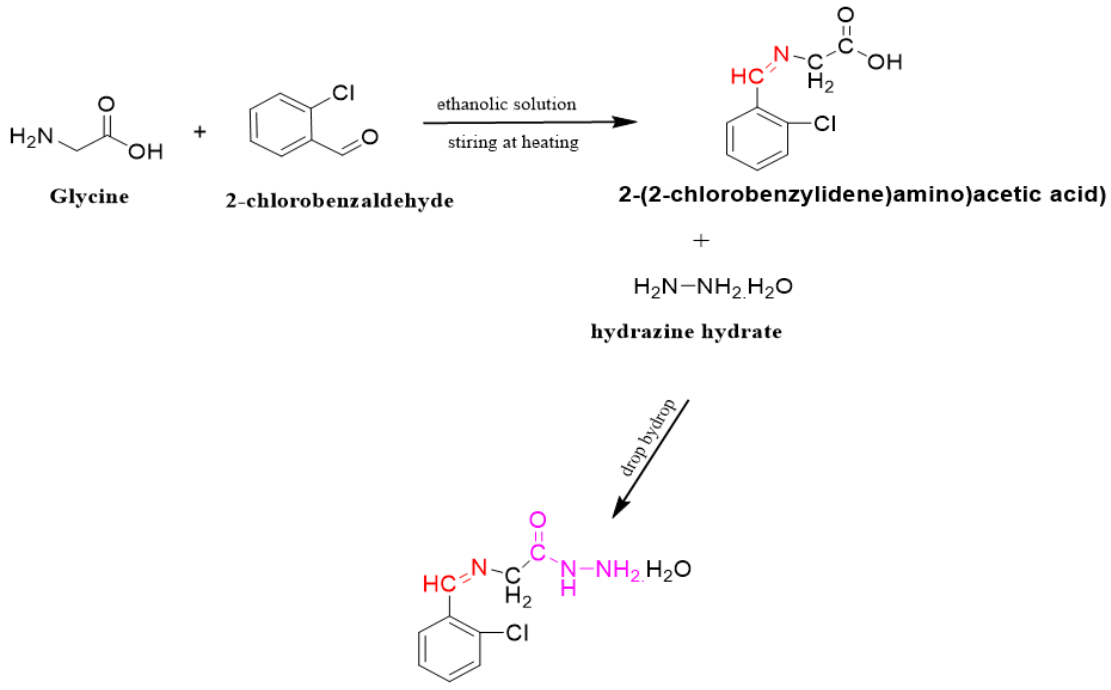

Figure 1. The schematic diagram of preparation of the ligand
Source: Elaborated by the authors using method from Gao (2013).

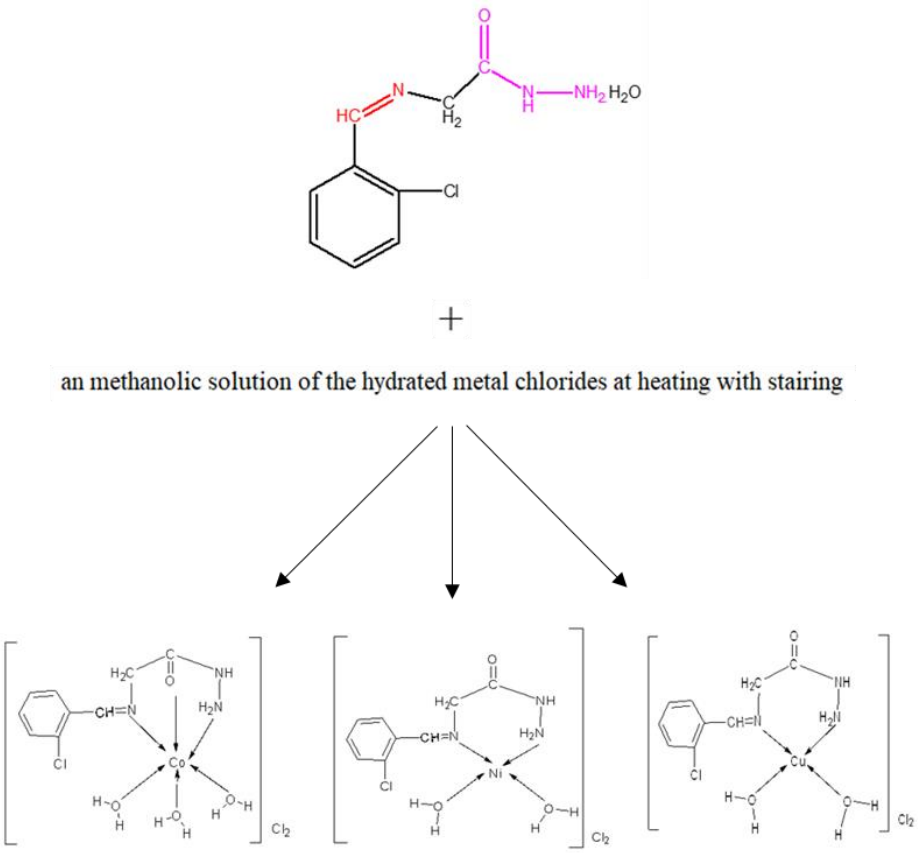

Figure 2. The schematic diagram of the synthesis method of the complexes.

Eclética Química, vol. 48, n. 1, 2023, 66-82
ISSN: 1678-4618
DOI: 10.26850/1678-4618eqj.v48.2.2023.p66-82

3. Results and discussion

All the compounds are colored solids and insoluble in common organic solvents except DMSO (Table 1). Molar conductance values of these compounds were in the range of 178–205 S cm^2 mol^{-1}, indicating their electrolytic nature (G. Mohamed *et al*., 2006) as recorded in Table 2.

Table 1. Some physical properties of the ligand and its complexes.

Complex Proposed Formula		L ($C_9H_{12}N_3O_2Cl$)	$[Co(L)(H_2O)_3]Cl_2$ $[Co(C_9H_{16}N_3O_4Cl)]Cl_2$	$[Ni(L)(H_2O)_2]Cl_2$ $[Ni(C_9H_{14}N_3O_3Cl)]Cl_2$	$[Cu(L)(H_2O)_2]Cl_2$ $[Cu(C_9H_{14}N_3O_3Cl)]Cl_2$
Color		Light brown	Purple	Green	Dark green
Melting point (°C)		142	160	285	295
Yield (%)		96.85	69.87	68.81	82.36
Solubility	dimethyl sulfoxide	soluble	soluble	soluble	soluble
	dimethylformamide	soluble	soluble	soluble	partially soluble
	diethyl ether	partially soluble	insoluble	insoluble	insoluble
	benzene	soluble	insoluble	insoluble	insoluble
	acetone	partially soluble	insoluble	insoluble	insoluble
	trichloromethane	soluble	insoluble	insoluble	insoluble
	tetrachloromethane	soluble	insoluble	insoluble	insoluble
	hexane	soluble	insoluble	insoluble	insoluble
	methanol	soluble	soluble	soluble	partially soluble
	ethanol	insoluble	soluble	partially soluble	partially soluble
	H_2O	insoluble	soluble	soluble	soluble

Table 2. Molecular weight, elemental analysis and molar conductance of the ligand and its complexes.

	Complex proposed formula	L	$[Co(L)(H_2O)_3]Cl_2$	$[Ni(L)(H_2O)_2]Cl_2$	$[Cu(L)(H_2O)_2]Cl_2$
Molecular weight	calc.	229.66	395.53	377.28	382.13
	found	229.69	395.56	377.29	382.14
%C	calc.	47.07	27.33	28.65	28.29
	found	47.07	27.33	28.65	28.29
%H	calc.	5.27	4.08	3.74	3.69
	found	5.28	4.09	3.74	3.70
%N	calc.	18.30	10.62	11.14	11
	found	18.29	10.62	11.14	11.02
%M	calc.	-	14.90	15.56	16.63
	found	-	14.90	15.56	16.64
%CI	calc.	15.43	26.89	28.19	27.83
	found	15.43	26.90	28.20	27.84
Molar Conductance (cm^2 mol^{-1} (Ω^{-1})	-	-	182	205	178

3.1 Molar ratio by conductivity measurements

Through the conductivity measurements of the ligand with the divalent metals Co(II), Ni(II) and Cu(II) in order to calculate the molar ratio between the ligand and these metals, the following was found:

1. The resulting values were high, indicating that these complexes have a conductive nature (Tulu and Yimer, 2018). This was also confirmed using silver nitrate;
2. The ratio between these metals and chloride ion was 1:2 (G. Mohamed *et al*., 2006), where the resulting values were located between 186.7–115.9 S cm^2 mol^{-1};
3. Through conductivity measurements for different concentrations of these complexes, conductivity readings were confirmed at a fixed molar value, which represents 1:1 between the ligand and these metals (Ghara *et al*., 2017) as show in Fig. 3.

Eclética Química, vol. 48, n. 1, 2023, 66-82
ISSN: 1678-4618
DOI: 10.26850/1678-4618eqj.v48.2.2023.p66-82

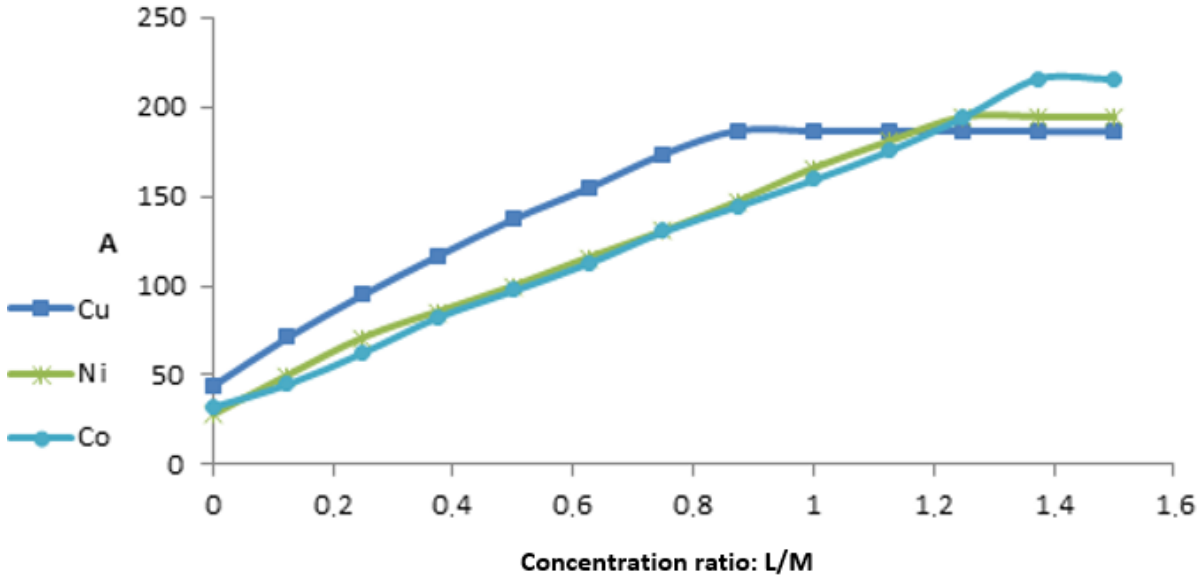

Figure 3. Curve of the mole ratio for the ligand and the metals.

3.2 IR spectra of the ligand and its complexes

Comparing the IR spectral data of the ligand and its complexes (Table 3 and Fig. 4) confirmed the complexation through the azomethine group $\upsilon_{C=N}$. The band at 1663 cm^{-1} assigned to $\upsilon_{C=N}$ in the free ligand was shifted to lower wave number in the complexes, indicating the participation of the azomethine nitrogen in coordination (Jamil *et al*., 2022; E. Mohamed *et al*., 2014). The IR spectra of the Co(II) complex showed a band at 1654 cm^{-1} which is characteristic of (C=O) group. This band is indicating coordination of this group through oxygen atom (Al-Salami *et al*., 2017). The band at 3106 cm^{-1} can be assigned to vibration of the NH_2 group in the ligand, which shifted to higher frequencies in the complexes, which identifies coordination of the amine nitrogen (Demirbaş *et al*., 2002).

The ligand and its complexes show additional broad bands in the range 3373–3436 cm^{-1} due to the OH stretching of the water molecule, which is confirmed by the elemental analysis and gravimetric studies (Al-Salami *et al*., 2017; Jamil *et al*., 2022). Low intensity bands observed in far-IR region in the range 528–591 cm^{-1} and 436–439 cm^{-1} which may probably be due to the formation M-O and M-N bonds, respectively (Alomari, 2010; Hossain *et al*., 2019).

Other absorption bands of v(N-N) (Ali *et al*., 1997; Dzulkifli *et al*., 2012), v(NH) (Ali *et al*., 1997; Ejelonu *et al*., 2018), v(Ar-Cl) (Emriye, 2016; Kapadnis *et al*., 2016), v(CH_2), v(C=C), (E. Mohamed *et al*., 2014), v(CH) (Al-Salami *et al*., 2017; E. Mohamed *et al*., 2014), v(NH_2) (Demirbaş *et al*., 2002) are given in Table 3.

Table 3. Significant IR spectral bands (cm^{-1}) of the ligand and its complexes.

Compounds	L	$[Co(L)(H_2O)_3]Cl_2$	$[Ni(L)(H_2O)_2]Cl_2$	$[Cu(L)(H_2O)_2]Cl_2$
C=N	1663^{w}	1616^{s}	1616^{s}	1617^{m}
C=O	1685^{w}	1654^{w}	1682^{w}	1685^{s}
C=C	1588^{m}	1588^{m}	1586^{m}	1580^{w}
C-N	1390^{m}	1412^{s}	1411^{s}	1411^{m}
NH	$3068^{w.br}$	$3068^{w.br}$	$3069^{w.br}$	3067^{w}
NH_2	3106^{br}	3347^{s}	3180^{w}	3250^{w}
=C-H	3033^{w}	3031^{w}	3032^{w}	$3030^{w.br}$
N-N	1047^{s}	1046^{s}	1045^{s}	1051^{m}
CH_2	1465^{s}	1464^{m}	1464^{m}	1458^{m}
Ph-Cl	869^{m}	868^{w}	863^{m}	870^{w}
OH	3432^{br}	3408^{br}	3373^{br}	3432^{br}
M-N	-	591^{m}	528^{m}	580^{w}
M-O	-	436^{m}	435^{m}	439^{w}

w = weak, m = medium, s = strong, br = broad.

Eclética Química, vol. 48, n. 1, 2023, 66-82
ISSN: 1678-4618
DOI: 10.26850/1678-4618eqj.v48.2.2023.p66-82

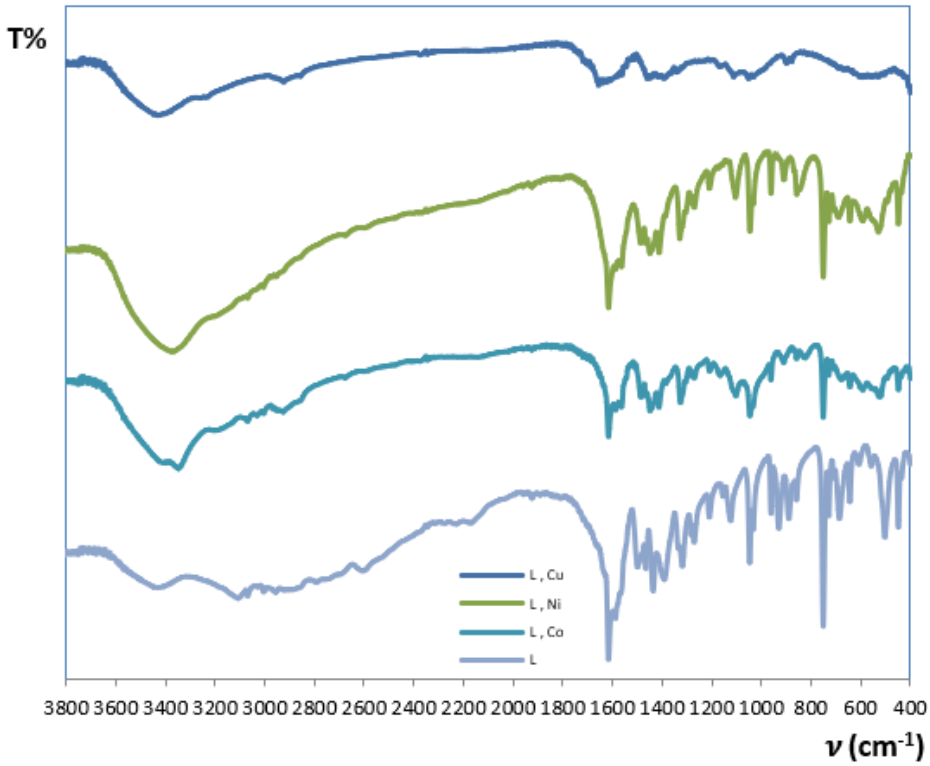

Figure 4. IR spectra of the ligand and its complexes.

3.3 NMR spectroscopy of the ligand

3.3.1 [1]HNMR

The resonance of protons has been assigned on the basis of their integration and multiplicity pattern. The [1]HNMR spectra of the ligand (Table 4 and Fig. 5) in DMSO exhibits signal at 8.55 ppm attributed to CH=N- proton (Al-Salami *et al*., 2015). The signals within the 6.85 and 6.88 ppm are assigned to the NH and NH_2 respectively (Mathew *et al*., 2006). Spectra of aromatic range was observed at 7.67–7.70 ppm (Sakhare *et al*., 2015). The signals appeared at 2.50 and 3.20 ppm were indicated the protons of CH_2 (Al-Garawi *et al*., 2012) and H_2O, respectively.

3.3.2 [13]C NMR

The [13]CNMR spectra provide further support for the structural characterization of the ligand (Table 4 and Fig. 6) [13]C NMR spectral data of the ligand has signal at 160.35 attributed to carbon of CH=N- (Neelofar *et al*., 2017). The aromatic carbon signals are present in the range 115.82–130.08 ppm (Oğuzhan *et al*., 2017). The [13]CNMR spectral data of the carbon amide and CH_2 group are present at 160.58 (Shneine *et al*., 2017) and 40.00 ppm (Neelofar *et al*., 2017), respectively. The structural formula of the ligand (Fig. 7).

Table 4. [1]H and [13]C NMR positions (ppm) of the ligand.

NMR Spectroscopy of the ligand			
[1]HNMR		**[13]C NMR**	
Site	**Chemical Shift (ppm)**	**Site**	**Chemical Shift (ppm)**
CH=N-	8.55	CH=N-	160.35
NH	6.85	A.R.	115.82-130.08
NH_2	6.88	CH_2	40.00
A.R.	7.67-7.70	C=O	160.58
CH_2	2.50	-	-
H_2O	3.20	-	-

Eclética Química, vol. 48, n. 2, 2023, 66-82
ISSN: 1678-4618
DOI: 10.26850/1678-4618eqj.v48.2.2023.p66-82

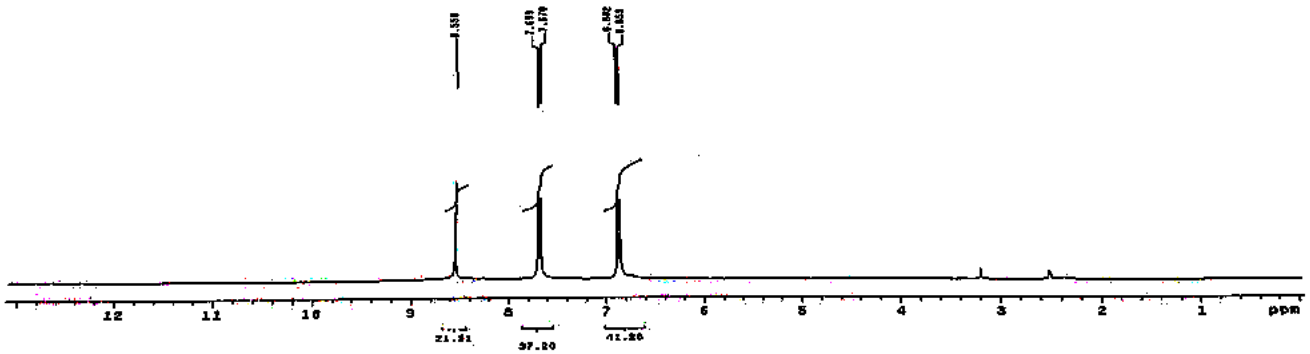

Figure 5. ^{1}HNMR spectrum of the ligand.

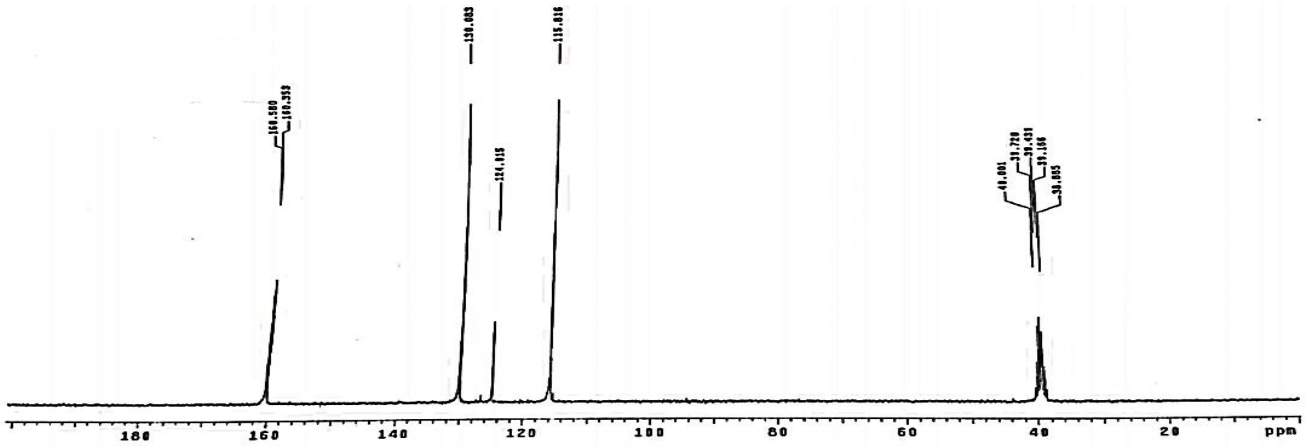

Figure 6. ^{13}CNMR spectrum of the ligand.

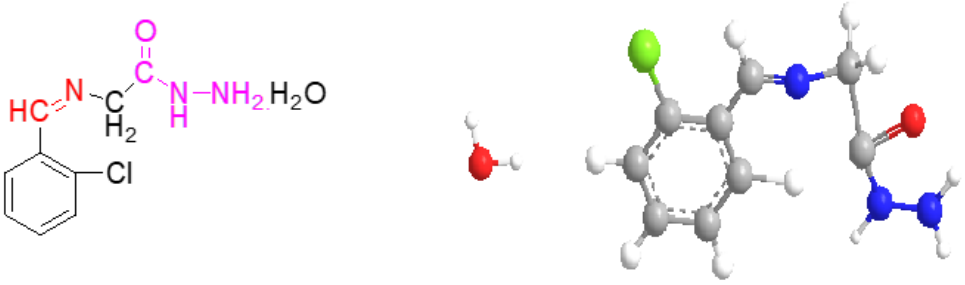

2-((2-chlorobenzylidene)amino)acetohydrazide hydrate = Ligand = L

Figure 7. The structural formula of the ligand.

3.4 Magnetic and electronic of the ligand and its complexes

The absorption spectrum of the ligand (Fig 11a) shows two absorption bands appearing at 45,454 and 33,333 cm^{-1}. The band appearing at low energy side at 33,333 cm^{-1} in the ligand is attributed to n-π* transitions of conjugation between the lone pair of electrons of p orbital of N-atom in C=N group and a conjugated π bond of aromatic rings (Hossain *et al.*, 2019). The band appearing at higher energy 45,454 cm^{-1} arise from π-π* transition within the phenyl and π-π* transitions of the C=N group (Sarwar *et al.*, 2018).

The electronic spectrum of the Co(II) complex as shown in Figs. 8 and 11b and Table 5, octahedral is suggested. This is based on the appearance of 13,513 cm^{-1} in the spectra recorded in DMSO solution, which is attributed to the $^{4}T_{1g} \rightarrow {}^{4}A_{2g}$ (ν_2) transitions (Patel *et al.*, 2012; Yousef *et al.*, 2016), also Co(II) complex has magnetic moment of 4.8 Bohr's magneton,

Eclética Química, vol. 48, n. 2, 2023, 66-82
ISSN: 1678-4618
DOI: 10.26850/1678-4618eqj.v48.2.2023.p66-82

BM, which lie in the range reported for octahedral geometry around the Co(II) ion (Sharma *et al*., 1994; Tulu and Yimer, 2018). Moreover, the purple color of the complex is in good agreement with this reported for octahedral Co(II) complex (Tulu and Yimer, 2018).

The magnetic measurements indicates that Ni(II) complex is a diamagnetic (Tulu and Yimer, 2018) and the electronic spectra of this complex in DMSO solution (Fig,11c and Table 5) showed two bands in 21,276 and 18,867 cm^{-1} attributed to $^1A_1g \rightarrow {}^1A_2$ g and $^1A_1g \rightarrow B_1g$ transitions, respectively, for square planar Ni(II) complex (Fig. 9) and the green color of this complex is additional evidence for square planar structure (Al-Jiboury and Al-Nama, 2019).

The electronic spectrum (Fig. 11d) of Cu(II) complex show one band at 21,730 cm^{-1}, assigned to the transitions $^2B_1g \rightarrow {}^2A_1g$, indicating square-planar geometry (Table 5 and Fig. 10) (Mahmood *et al*., 2013). This geometry is further supported as the values of the magnetic moment obtained 1.87 B.M, which is lying in the range reported for a square-planar structure (Mahmood *et al*., 2013; Mishra *et al*., 2012). The green color of this complex is additional evidence for square planar structure (Mahmood *et al*., 2013).

Also, the bands at 24,390, 22,222, and 24,691 cm^{-1} should be attributed to the charge transfer of Co(II) (Mahmood *et al*., 2013), Ni(II) (G. Mohamed *et al*., 2006) and Cu(II) complexes (Hossain *et al*., 2019), respectively.

Table 5. Magnetic moment, electronic spectral data in DMSO solution for the ligand and its complexes.

Compounds		L	$[Co(L)(H_2O)_3]Cl_2$	$[Ni(L)(H_2O)_2]Cl_2$	$[Cu(L)(H_2O)_2]Cl_2$
μ_{eff} (B.M.)		-	2.6	-	1.87
UV bands (cm^{-1})	π→π*	45,454	-	-	-
	n→π*	33,333	-	-	-
Charge transfer bands (cm^{-1})		-	24,390	22,222	24,691
d-d transition bands (cm^{-1})		-	13,513	18,867, 21,276, 13,698	21,739
Supposed structure		-	Octahedral	Square planar	Square planar

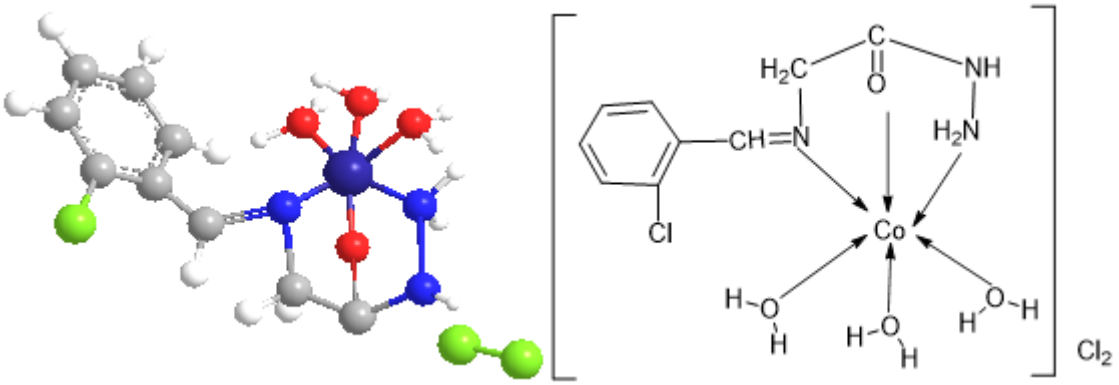

Figure 8. Complex containing the ligand with Co(II).

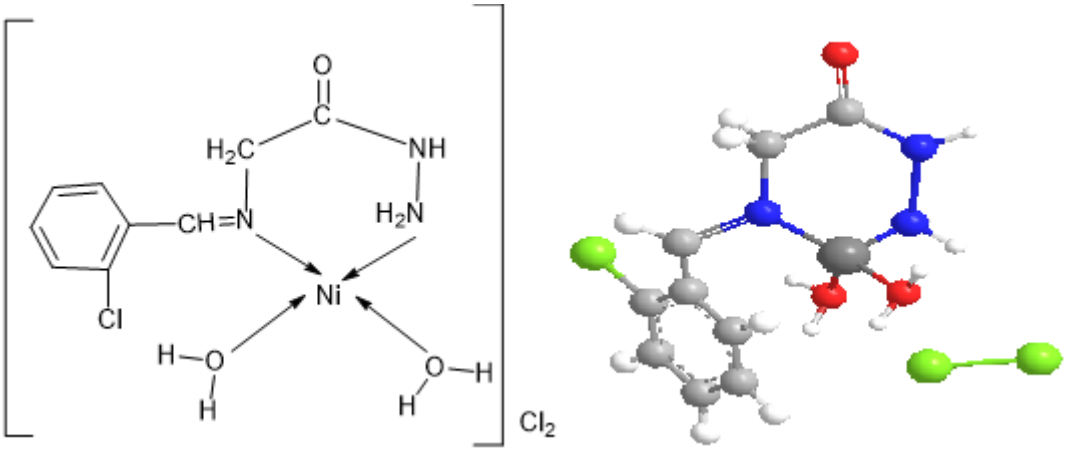

Figure 9. Complex of the ligand with Ni(II).

Eclética Química, vol. 48, n. 2, 2023, 66-82
ISSN: 1678-4618
DOI: 10.26850/1678-4618eqj.v48.2.2023.p66-82

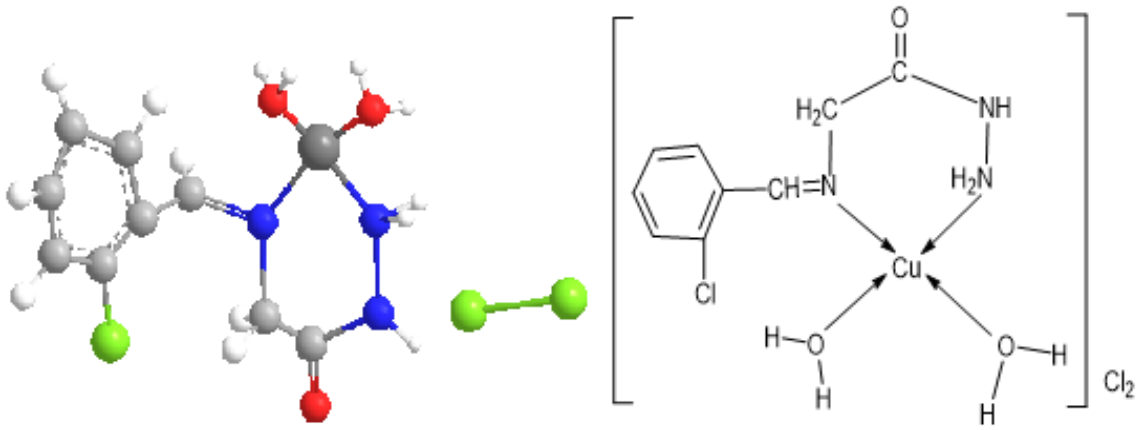

Figure 10. Complex of the ligand with Cu(II).

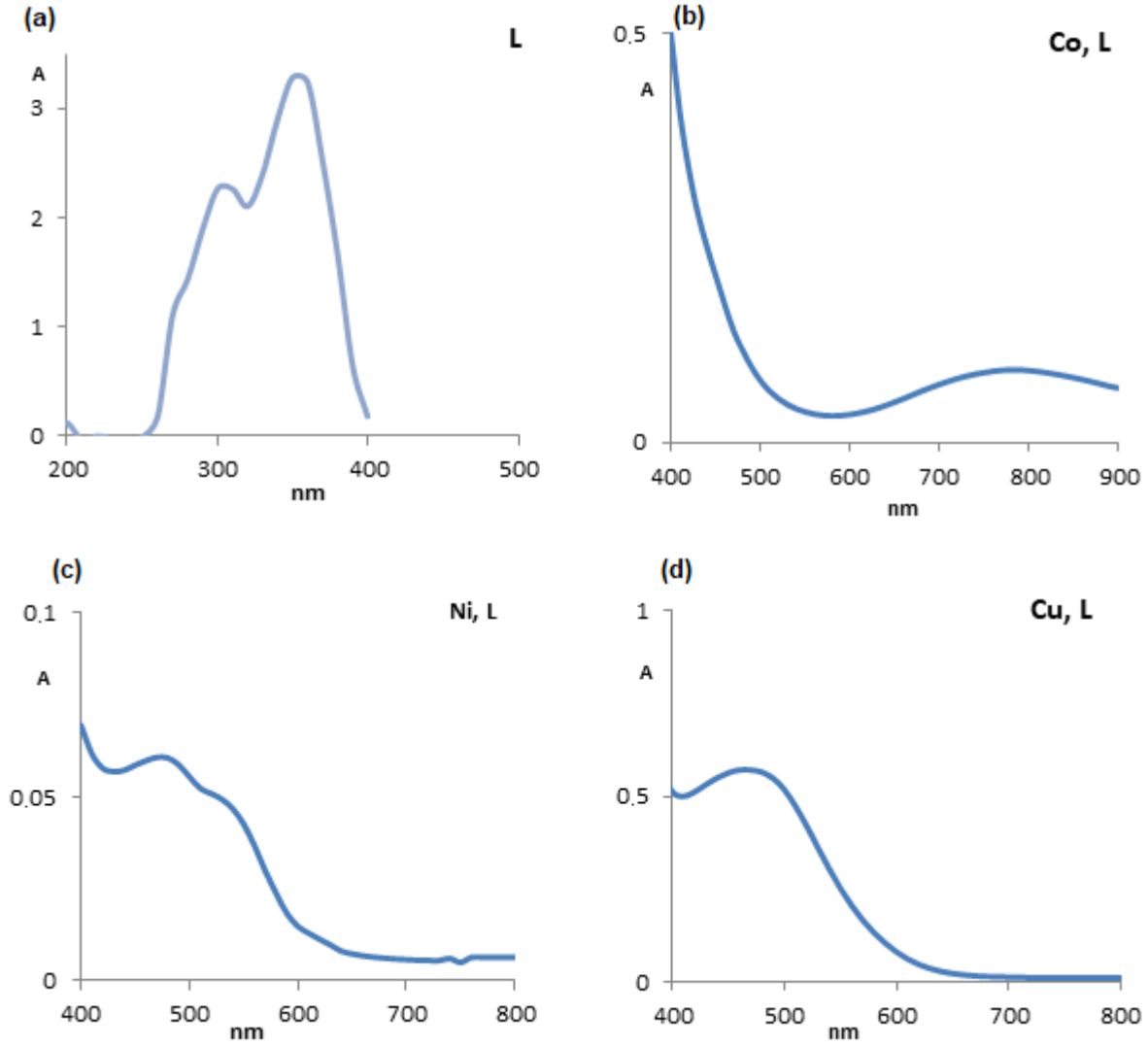

Figure 11. UV-visible electronic spectra of the ligand and its complexes in DMSO solution. **(a)** for the ligand; **(b)** for the Co complex; **(c)** for the Ni complex; **(d)** for the Cu complex.

Eclética Química, vol. 48, n. 2, 2023, 66-82
ISSN: 1678-4618
DOI: 10.26850/1678-4618eqj.v48.2.2023.p66-82

3.5 Powder X-ray diffraction of the ligand and its complexes

The powder X-ray powder diffraction patterns for the free ligand and its complexes were carried out in order to obtain an idea about the lattice dynamics of the resulted complexes. X-ray of these compounds are recorded and shown in Figs. 12 and 13.

The values of particle size, strain and relative intensity (%) of compounds are compiled in Table 6. The crystallite size could be estimated from X-ray diffraction (XRD) patterns by applying full width at half maximum (FWHM) of the characteristic peaks using Debye-Scherrer Eq. 1 (Al-Maydama *et al*., 2018; Refat *et al*., 2014a; b) and Williamson-Hall Eq. 2 (Abed *et al*., 2019).

$$D = K\lambda/\beta \cos\theta \quad (1)$$

$$D = K\lambda/intercept \quad (2)$$

where $\boldsymbol{K}$ is Scherrer constant and equals 0.94, $\boldsymbol{\lambda}$ is the X-ray wavelength of Cu-Kα radiation (0.15405 nm), $\boldsymbol{\beta}$ is FWHM, and $\boldsymbol{\theta}$ is Bragg diffraction angle in radian. The particle size of these compounds is located within the nano scale range (12.59–35.32 nm).

The strain calculated by applying Williamson-Hall Eq. 2 (Abed *et al*., 2019) which mean the slope as Eq. 3.

$$Strain\ (\varepsilon) = \beta \cos\theta\ /\ \sin\theta \quad (3)$$

It was shown through crystal strain from William's equation that the ligand, Co(II) and Cu(II) complexes have the property of crystal tensile, while the Ni(II) complex has the property of crystal compressive, which corresponds to the size of the crystals. It was found that the higher the compressive which negative values, the smaller the crystal size, while the higher the tensile with positive values, the higher the crystal size, and this is what was clarified in Table 6.

The percentage of crystallinity, $X_c(\%)$, was calculated on the basis of the integrated peak areas of the principal peaks (Al-Maydama *et al*., 2018). The crystallinity of the complex is calculated relative to the crystallinity of the ligand as a ratio (Eq. 4).

$$X_C(\%) = \frac{A_{complex}}{A_{ligand}} \times 100 \quad (4)$$

where $A_{complex}$ and A_{ligand} are the areas under the principal peaks of the complex and the ligand sample, respectively. The results of these calculations were that the crystalline percentage of the Ni(II) complex is high compared to the ligand, while it was low for the Co(II) and Cu(II) complexes when compared to the ligand.

Table 6. XRD spectral data of the highest value of intensity of the ligand and its complexes.

Compounds	Θ (Radian)	B(FWHM) (Radian)	βcosθ	4sinθ	D(nm)	Scherr Mean D(nm)	W-H D(nm)	Strain (ε) *10^{-4}	X%
L	0.1744	0.004660	0.004589	0.6939	31.55	26.66	31.48	11	100
	0.2047	0.006842	0.006699	0.8132	21.62				
	0.2381	0.005498	0.005343	0.9433	27.11				
	0.2656	0.005690	0.005490	10.501	26.38				
[Co(L)(H$_2$O)$_3$]Cl$_2$	0.1735	0.008116	0.007994	0.6905	18.12	21.87	20.40	0.2	80.66
	0.2000	0.004721	0.004636	0.7947	31.24				
	0.2311	0.009564	0.009310	0.9161	15.55				
	0.2663	0.006651	0.006415	10.528	22.57				
[Ni((L)(H$_2$O)$_2$]Cl$_2$	0.1737	0.008186	0.008062	0.6912	17.96	20.76	12.59	–49	130.79
	0.2068	0.006650	0.006508	0.8214	22.25				
	0.2323	0.008796	0.008560	0.9209	16.92				
	0.2665	0.005794	0.005590	10.535	25.91				
[Cu(L)(H$_2$O)$_2$]Cl$_2$	0.1744	0.00481	0.004727	0.6939	30.64	28	35.32	16	75.99
	0.2133	0.005515	0.005390	0.8467	26.87				
	0.2372	0.007871	0.007651	0.9399	18.93				
	0.2554	0.004206	0.004061	10.103	35.59				

Eclética Química, vol. 48, n. 1, 2023, 66-82
ISSN: 1678-4618
DOI: 10.26850/1678-4618eqj.v48.2.2023.p66-82

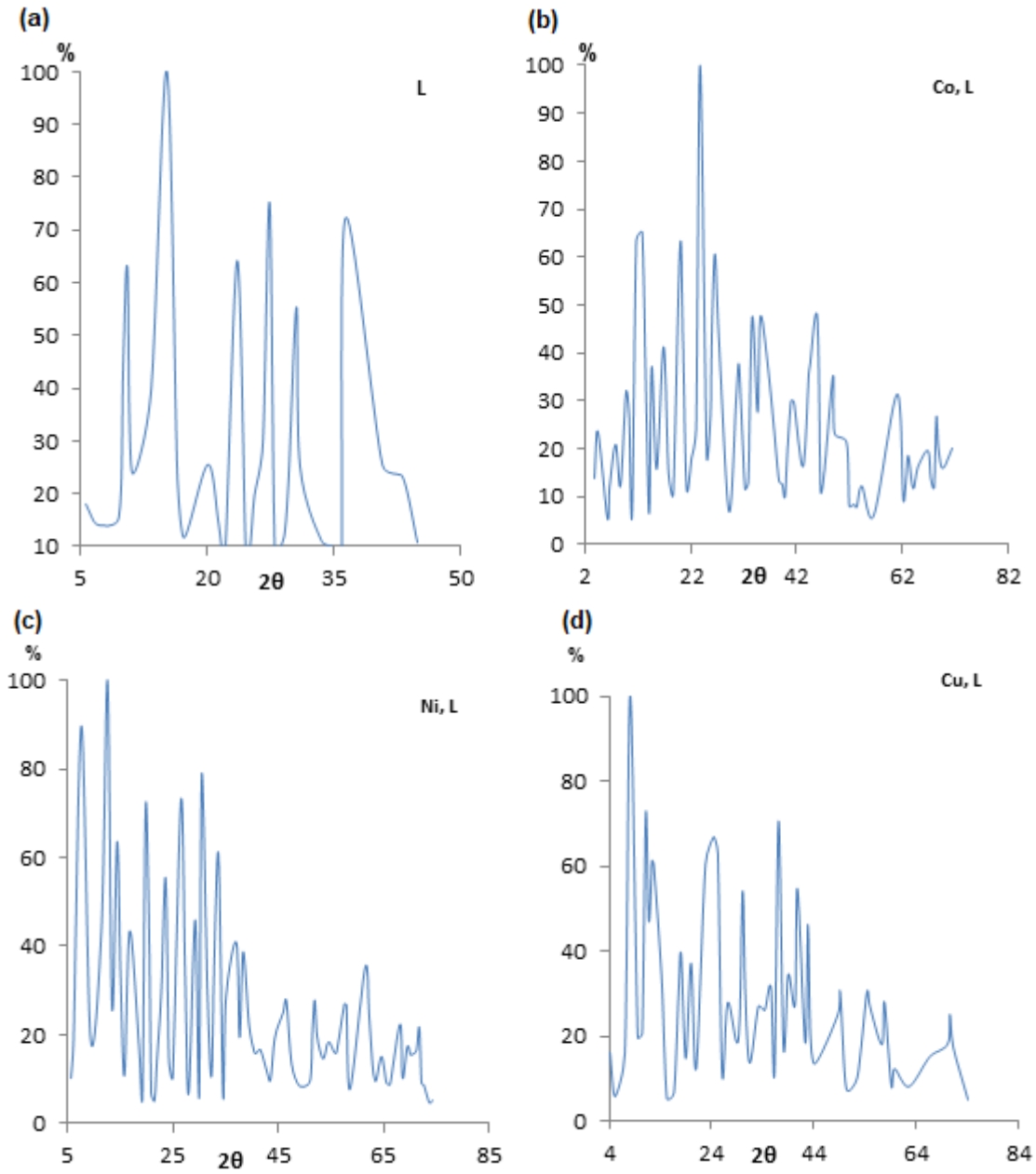

Figure 12. XRD patterns of the ligand and its complexes. **(a)** for the ligand; **(b)** for the Co complex; **(c)** for the Ni complex; **(d)** for the Cu complex.

Eclética Química, vol. 48, n. 2, 2023, 66-82
ISSN: 1678-4618
DOI: 10.26850/1678-4618eqj.v48.2.2023.p66-82

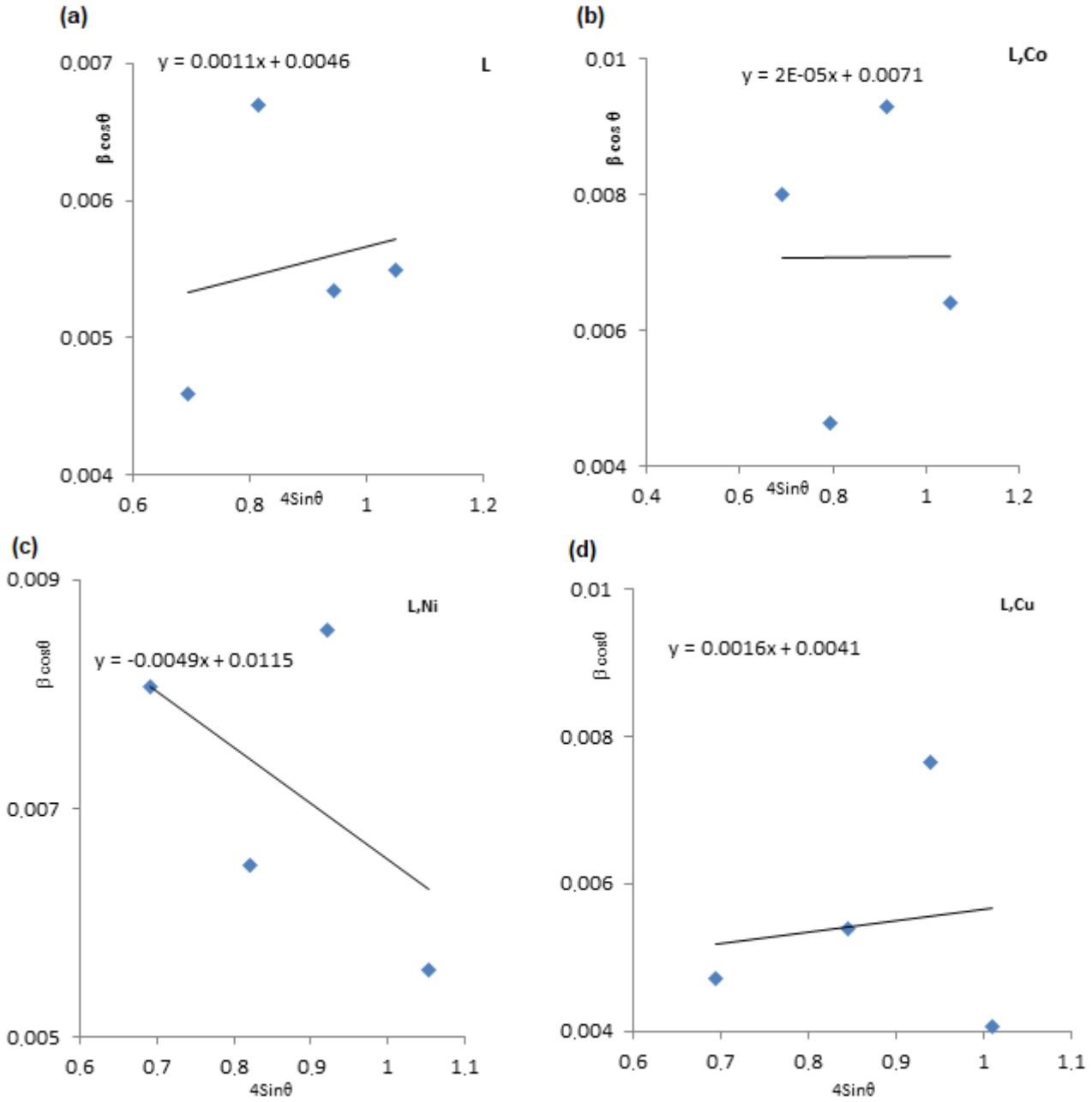

Figure 13. Particle size and strain by W-H of the ligand and its complexes. **(a)** for the ligand; **(b)** for the Co complex; **(c)** for the Ni complex; **(d)** for the Cu complex.

3.6 The ligand as antioxidant

The 2((2-chlorobenzylidene)amino)acetohydrazide hydrate=(L) has been synthesized, and the antioxidant properties were studied using ferric-bipyridine reducing capacity of total antioxidants method (Naji *et al*., 2020). As it was found that this ligand can be used as an antioxidant compared to ascorbic acid, which was used as a standard material in this analysis, but with less effectiveness than ascorbic acid, which gave 3.7453 mg compared with ascorbic acid, which was 1 mg, while the standard deviation of this ligand was ± 9.67 × 10^{-8}.

3.7 Antimicrobial of the ligand and its complexes

This analysis of the ligand and its mineral complexes clearly demonstrated that they have antibacterial and antifungal activity (Table 7, Figs. 14 and 15).

Comparison of the biological evaluation of the ligand and its complexes with standards of gentamicin (antibacterial agent), nystatin, miconazole, itraconazole

Eclética Química, vol. 48, n. 2, 2023, 66-82
ISSN: 1678-4618
DOI: 10.26850/1678-4618eqj.v48.2.2023.p66-82

and metronidazole (antifungal agents). The results of the highest-to-lowest-impact items can be summarized as follows:

a. *Staphylococcus aureus*
Ni > Co > Cu > ligand

b. *Bacillus subtilis*
Co > Cu > Ni > ligand

c. *Pseudomonas aeruginosa*
Co > Ni > ligand > Cu

d. *Escherichia coli*
Ni > ligand > Cu

e. *Aspergillus flavus*
Ni > Co > Cu > ligand

f. *Candida albicans*
ligand = Co > Ni > Cu

From these results, we can summarize that:

1. Generally, the active property of the free ligand and complexes against the used strains is enhanced;
2. The growth of *S. aureus* and *A. flavus* are inhibited by complex of Ni(II), Co(II), Cu(II), and the ligand, respectively;
3. *Bacillus subtilis* is inhibited by complex of Co(II) more than complexes of Cu(II), Ni(II) and the ligand. The growth of *E. coli* is just inhibited by complex of Ni(II), the ligand and complex of Cu(II) compared to the complex of Co(II) there is no inhibition;
4. The Inhibition zone of Co(II) complex toward *P. aeruginosa* was more than that of Ni(II), Cu(II) complexes and the ligand.
5. The ligand and complex of Co(II) have the same worthy effect against *C. albicans*, which are more than complexes of Ni(II) and Cu(II).

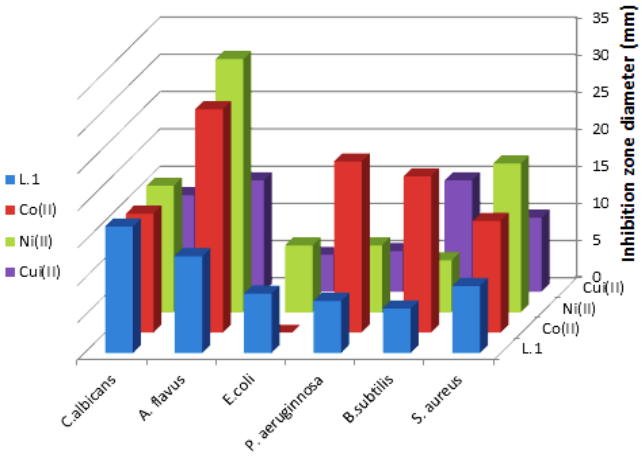

Figure 14. Diagram effect of the ligand and its complexes on the growth of bacteria and fungi (zone of inhibition in mm).

Table 7. Effect of the ligand and its complexes on the growth of bacteria and fungi (zone of inhibition in mm).

Compound (1000 µg mL^{-1})			Inhibition zone diameter (mm)					
			Bacteria				fungi	
			Gram positive		Gram negative			
			Staphylococcus aureus	*Bacillus subtilis*	*Pseudomonas aeruginosa*	*Escherichia coli*	*Aspergillus flavus*	*Candida albicans*
Control DMSO			0.0	0.0	0.0	0.0	0.0	0.0
Standard	Antibacterial agent Gentamicin 120 µg mL^{-1}		23	22	25	23	-	-
	Antifungal agent	Nystatin 100 µg mL^{-1}	-	-	-	-	25	**21**
		Miconazole 50 µg mL^{-1}	-	-	-	-	8	**22**
		Itraconazole 30 µg mL^{-1}	-	-	-	-	18	**20**
		Metronidazole 5 µg mL^{-1}	-	-	-	-	10	**17**
L			9	6	7	8	13	17
$[Co(L)(H_2O)_3]Cl_2$			15	21	23	0	30	16
$[Ni(L)(H_2O)_2]Cl_2$			20	7	9	9	34	17
$[Cu(L)(H_2O)_2]Cl_2$			10	15	5.5	5	15	13

Eclética Química, vol. 48, n. 2, 2023, 66-82
ISSN: 1678-4618
DOI: 10.26850/1678-4618eqj.v48.2.2023.p66-82

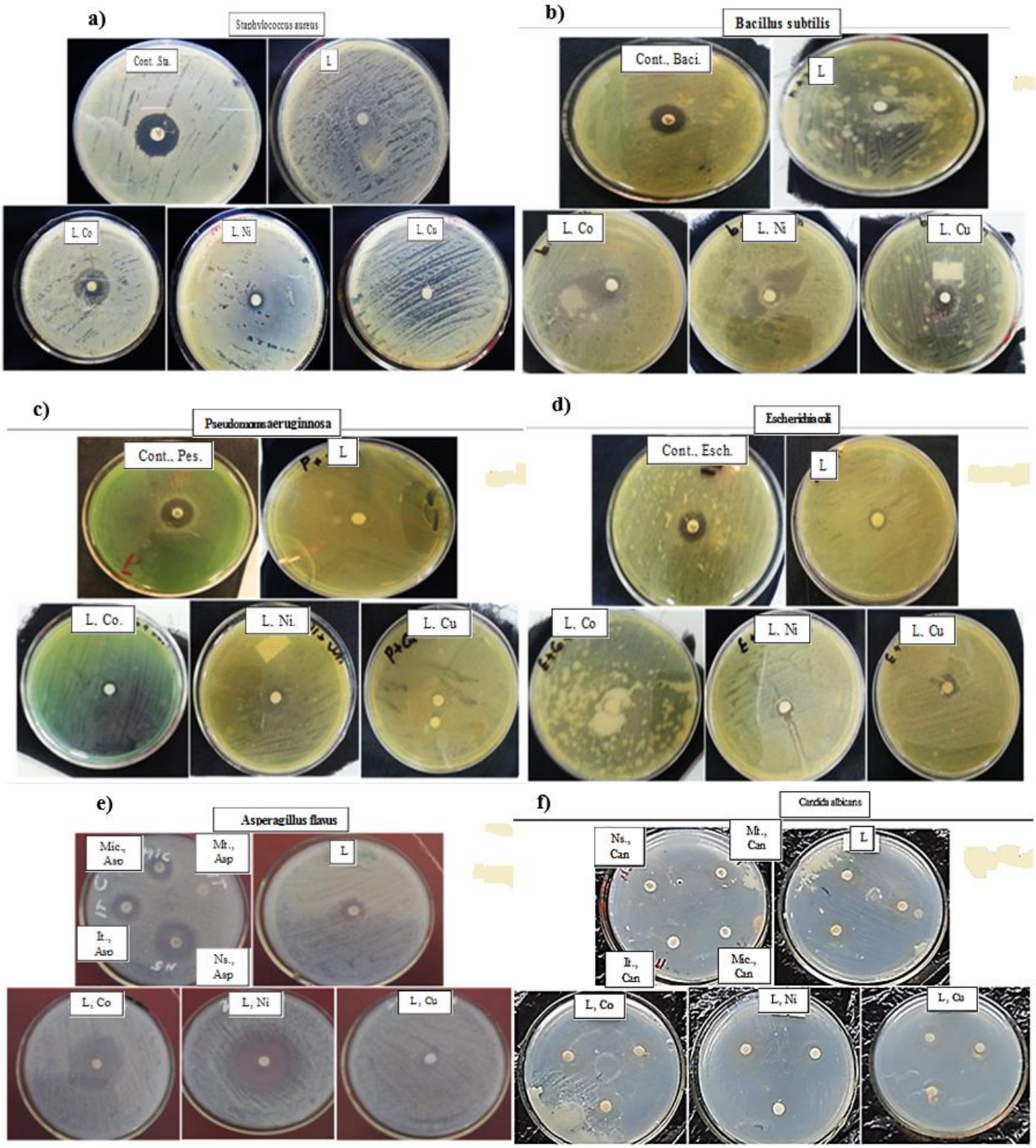

Figure 15. Biological activity of the ligand and its complexes . against **(a)** *Staphylococcus aureus*; **(b)** *Bacillus subtilis* **(c)** *Pseudomonas aeruginosa*; **(d)** *Escherichia coli*; **(e)** *Bacillus subtilis*; **(f)** *Pseudomonas aeruginosa*.

According to the concept of cell permeability, since the lipid membrane that surrounds the cell favors the passage of lipid-soluble substances since lipid solubility is an important factor, so the polarity of the metal ion is greatly reduced due to the overlap of the orbitals of the metal ion with the bound. It increases the delocalization of electrons on the chelated rings and enhances the lipophilicity of the complexes, which facilitates the

Eclética Química, vol. 48, n. 2, 2023, 66-82
ISSN: 1678-4618
DOI: 10.26850/1678-4618eqj.v48.2.2023.p66-82

penetration of the lipid membranes of microorganisms and facilitates the closure of the metal bonding sites with enzymes.

These compounds deactivate various cellular enzymes, which play a vital role in the various metabolic pathways of these organisms. It has also been suggested that the final action of the toxin is denaturation of one or more cell proteins, impairing normal cellular processes (Jamil *et al*., 2022; Omer and Al-Daher, 2019; Refat *et al*., 2015; Reiss *et al*., 2021).

4. Conclusions

The Schiff base hydrazide ligand derived from the condensation of 2-chlorobenzaldehyde, glycine and hydrazine hydrate have been successfully synthesized. These ligand were complexed with using Co(II), Ni(II) and Cu(II) ions. Coordination of amine nitrogen (-NH_2) and azomethine nitrogen (-C=N-) with Ni(II) and Cu(II) in additional to oxygen of carbonyl group with Co(II). These compounds have been indicated by various studies; hence, it has been liable for imparting the stability to the complexes. The structures of these compounds were characterized by elemental, ^{1}HNMR, ^{13}CNMR, FTIR spectra, molar ratio, XRD diffraction, UV-Vis spectra, and magnetic studies. The coordination of the ligand with Co(II), Ni(II) and Cu(II) ions showed molar ratio of 1:1. The complexes of Co(II) and Cu(II) presented square planar geometries, while Ni(II) presented octahedral geometry. Antioxidant study for the ligand provided its activity. The ligand with Schiff base and hydrazide groups and its complexes showed better biological activity. The results showed that the metal complexes have much higher antibacterial and antifungal activity compare to the parent ligand. It was found that the Co(II) complex was more effective than other metal complexes used against all types of bacteria and it was more effective against *P. aeruginosa* with diameter inhibition zone of 23 mm, while Ni(II) complex was more effective than other complexes used against two types of fungi and it was more effective against *A. flavus* than *C. albicans.*

Authors' contribution

Conceptualization: Al-Azab, F. M.; Jamil, Y. M.
Data curation: Al-Azab, F. M.; Jamil, Y. M.; Al-Gaadbi, A. A.
Formal Analysis: Al-Azab, F. M.; Jamil, Y. M.; Al-Gaadbi, A. A.
Funding acquisition: Not applicable.
Investigation: Al-Azab, F. M.; Jamil, Y. M.; Al-Gaadbi, A. A.
Methodology: Jamil, Y. M.; Al-Azab, F. M.
Project administration: Jamil, Y. M.; Al-Azab, F. M.
Resources: Al-Azab, F. M.; Jamil, Y. M.; Al-Gaadbi, A. A.
Software: Jamil Y. M.; Al-Gaadbi A. A.
Supervision: Al-Azab, F. M.; Jamil, Y. M.
Validation: Al-Azab, F. M.
Visualization: Al-Azab, F. M.; Jamil, Y. M.; Al-Gaadbi, A. A.
Writing – original draft: Al-Gaadbi, A. A.
Writing – review & editing: Jamil, Y. M.

Data availability statement

All data sets were generated or analyzed in the current study.

Funding

Not applicable.

Acknowledgments

Not applicable.

References

Abed, A. H.; Khodair Z. T.; Al-Saadi, T. M.; Al-Dhahir, T. A. Study the evaluation of Williamson–Hall (W-H) strain distribution in silver nanoparticles prepared by sol-gel method. *AIP Conf. Proc.* **2019**, *2123* (1), 020019. https://doi.org/10.1063/1.5116946

Al Zoubi, W. Biological Activities of Schiff Bases and Their Complexes: A Review of Recent Works. *Int. J. Org. Chem.* **2013**, *3* (3A), 73–95. https://doi.org/10.4236/ijoc.2013.33A008

Al-Garawi, Z. S. M.; Tomi, I. H. R.; Al-Daraji, A. H. R. Synthesis and characterization of new amino acid-Schiff bases and studies their effects on the activity of ACP, PAP and NPA enzymes (*In Vitro*). *J. Chem.* **2012**, *9* (2), 962–969. https://doi.org/10.1155/2012/218675

Ali, M. A.; Majumder, S. M. M.-u.-H.; Butcher, R. J.; Jasinski, J. P.; Jasinski, J. M. The preparation and characterization of bis-chelated nickel(II) complexes of the 6-methylpyridine-2-carboxaldehyde Schiff bases of S-alkyldithiocarbazates and the X-ray crystal structure of the bis {S-methyl-*β*-*N*-(6-methylpyrid-2-yl)- methylenedithiocarbazato}nickel(II) complex. *Polyhedron* **1997**, *16* (16), 2749–2754. https://doi.org/10.1016/S0277-5387(97)00036-3

Eclética Química, vol. 48, n. 2, 2023, 66-82
ISSN: 1678-4618
DOI: 10.26850/1678-4618eqj.v48.2.2023.p66-82

Al-Jiboury, M. M.; Al-Nama, K. S. Preparation, Characterization and Biological Activities of some Unsymmetrical Schiff bases derived from m-phenyelenediamine and their metal complexes. *Raf. J. Sci.* **2019**, *28* (2), 23–36. https://doi.org/10.33899/rjs.2019.159965

Al-Maydama, H. M.; Abduljabbar, A. A.; Al-Maqtari, M. A.; Naji, K. M. Study of temperature and irradiation influence on the physicochemical properties of aspirin. *J. Mol. Struct.* **2018**, *1157*, 364–373. https://doi.org/10.1016/j.molstruc.2017.12.062

Alomari, A. A. Synthesis, characterization and electrochemical studies of Cu(II), Fe(II), Fe(III) and Ni(II) complexes of Someo-phenylenediamine Schiff base. Master's Thesis, University of Malaya Kuala Lumpur, Kuala Lumpur, 2010.

Al-Salami, B. K.; Gata, R. A.; Asker, K. A. Synthesis Spectral, Thermal Stability and Bacterial Activity of Schiff Bases Derived from Selective Amino Acid and Their Complexes. *Adv. Appl. Sci. Res.* **2017**, *8* (3), 4–12.

Al-Salami, B. K.; Ul-Saheb, R. G. A.; Asker, K. A. Synthesis spectral, thermal stability and antibacterial activity of schiff bases derived from alanine and threonine and their complexes. *J. Chem. Pharm. Res.* **2015**, *7* (8), 792–803.

Ashraf, M. A.; Mahmood, K.; Wajid, A. Synthesis, Characterization and Biological Activity of Schiff Bases. *IPCBEE*. **2011**, *10*, 1–7.

Demirbaş, N. Demirbaş, A.; Sancak, K. Synthesis and characterization of some 3-alkyl-4-amino-5-cyanomethyl-4H-1,2,4-triazoles. *Turk J. Chem.* **2002**, *26*, 801–806.

Dzulkifli, N. N.; Farina, Y.; Baba, I.; Ibrahim, N. Synthesis, structural, antibacterial and spectral studies of Co(II) complexes with salicylaldehyde and *p*-chlorobenzaldehyde 4-phenylthiosemicarbazone. *Malaysian J. Anal. Sci.* **2012**, *16* (2), 103–109.

Ejelonu, B. C.; Oyeneyin, O. E.; Olagboye, S. A.; Akele, O. E. Synthesis, characterization and antimicrobial properties of transition metal complexes of aniline and sulphadiazine Schiff bases as mixed ligands. *J. Chem. Pharm. Res.* **2018**, *10* (5), 67–73.

Emriye, A. Y. Synthesis and characterization of Schiff base 1-Amino-4-methylpiperazine derivatives. *CBU J. of Sci*. **2016**, *12* (3), 375–392.

Gao, H. Synthesis, Characterisation and transition metal ion complexation studies of "pocket-like" imine and amide derivatives. Doctoral Dissertation, National University of Ireland Maynooth, Maynooth, 2013.

Ghara, A.; Si, A.; Majumder, M.; Bagchi, A.; Raha, A.; Mukherjee, P.; Pal, M.; Saha, R.; Bassu, S. A detailed study of Transition Metal Complexes of a Schiff base with its Physico-chemical properties by using an electrochemical method. *AJPP*. **2017**, *3* (3), 86–94.

Hossain, S.; Banu, L. A.; E-Zahan, K.; Haque, M. Synthesis, characterization and biological activity studies of mixed ligand complexes with Schiff base and 2,2-bipyridine. *Int. J. Appl. Sci. Res. Rev.* **2019**, *6* (1–2), 1–7.

Jamil, Y. M. S.; Al-Azab, F. M.; Al-Selwi, N. A.; Alorini, T.; Al-Hakimi, A. N. Preparation, physicochemical characterization, molecular docking and biological activity of a novel Schiff-base and organophosphorus Schiff base with some transition metal(II) ions. *Main Group Chemistry* **2022**, *Pre-press*, 1–26. https://doi.org/10.3233/MGC-220101

Kapadnis, K. H.; Jadhav, S. P.; Patil, A. P.; Hiray, A. P. Four synthesis methods of Schiff base ligands and preparation of their metal complex with Ir and antimicrobial investigation. *WJPPS.* **2016**, *5* (2), 1055–1063.

Mahmood, T. H.; Hassan, E. A.; Mubark, L. A. Preparation and characterization of Co(II), Ni(II) and Cu(II) ions binuclear complexes with macrocyclic Schiff base derived from acidhydrazide and α-hydroxy ketone. *JUAPS.* **2013**, *7* (2).

Majumdar, P.; Pati, A.; Patra, M.; Behera, R. K.; Behera, A. K. Acid hydrazides, potent reagents for synthesis of oxygen-, nitrogen-, and/or sulfur-containing heterocyclic rings. *Chem. Rev.* **2014**, *114* (5), 2942–2977. https://doi.org/10.1021/cr300122t

Malakyan, M.; Babayan, N.; Grigoryan, R.; Sarkisyan, N.; Tonoyan, V.; Tadevosya, D.; Matosyan, V.; Aroutiounian, R.; Arakelyan, A. Synthesis, characterization and toxicity studies of pyridinecarboxaldehydes and L-tryptophan derived Schiff bases and corresponding copper (II) complexes. *F1000 Research*. **2016**, *5*, 1921. https://doi.org/10.12688/f1000research.9226.1

Mathew, G.; Susselan, M. S.; Krishnan, R. Synthesis and characterisation of cobalt (II) complexes of chromen-2-one-3-carboxy hydrazide and 2-(chromen-2-onyl)-5-(aryl)1,3,4-oxadiazoe derivatives. *Indian J. Chem.* **2006**, *45A*, 2040–2044.

Mishra, A. P.; Sharma, N.; Jain, R. K. Microwave Synthesis, Spectral, Thermal and antimicrobial studies of some Ni(II) and Cu(II) Schiff base complexes. *Avances en Química* **2012**, *7* (1), 77–85.

Mohamed, E. A.; Mohamed, B.; Mustapha, H. Synthesis and characterization of N-salicylidèneglycinate (KHL) and caffeine complexes with Cd (II), Cu (II), Ni (II), Zn (II). *IJCPS*. **2014**, *3* (5), 22–34.

Mohamed, G. G.; Omar; M. M.; Hindy, A. M. Metal Complexes of Schiff Bases: Preparation, Characterization and Biological Activity. *Turk J. Chem*. **2006**, *30*, 361–382.

Naji, K. M.; Thamer, F. H.; Numan, A. A.; Dauqan, E. M.; Alshaibi, Y. M.; D'souza, M. R. Ferric-bipyridine assay: A novel spectrophotometric method for measurement of

Eclética Química, vol. 48, n. 2, 2023, 66-82
ISSN: 1678-4618
DOI: 10.26850/1678-4618eqj.v48.2.2023.p66-82

antioxidant capacity. *Heliyon.* **2020**, *6* (1), E03162. https://doi.org/10.1016/j.heliyon.2020.e03162

Neelofar, N. A.; Khan, A.; Amir, S.; Khan, N. A.; Bilal, M. Synthesis of Schiff bases derived from 2-hydroxy-1-naphthaldehyde and their tin(II) complexes for antimicrobial and antioxidant activities. *Bull. Chem. Soc. Ethiop.* **2017**, *31* (3), 445–456. https://doi.org/10.4314/bcse.v31i3.8

Oğuzhan, B.; Campolat, E.; Şahal, H.; Kaya, M. The synthesis, characterization of a novel Schiff base ligand and investigation of its transition metal complexes. *Adyu. J. Sci*. **2017**, *7* (1), 47–59.

Omer, D. A.; Al-Daher, A. G. M. New tridentate hydrazone metal complexes derived from 2-hydroxy-4-methoxyacetophenone and some acid hydrazides: synthesis, characterization and antibacterial activity evaluation. *Raf. J. Sci.* **2019**, *28* (2), 100–111. https://doi.org/10.33899/rjs.2019.159969

Patel, K. S.; Patel, J. C.; Dholariya, H. R.; Patel, V. K.; Patel, K. D. Synthesis of Cu(II), Ni(II), Co(II), and Mn(II) Complexes with Ciprofloxacin and Their Evaluation of Antimicrobial, Antioxidant and Anti-Tubercular Activity. *Open J. Met.* **2012**, *2* (3), 49–59. https://doi.org/10.4236/ojmetal.2012.23008

Refat, M. S.; Al-Maydama, H. M. A.; Al-Azab, F. M.; Amin, R. R.; Jamil, Y. M. S. Synthesis, thermal and spectroscopic behaviors of metal – drug complexes: La (III), Ce(III), Sm(III) and Y(III) amoxicillin trihydrate antibiotic drug complexes. *Spectrochim. Acta A Mol. Biomol. Spectrosc*. **2014a**, *128*, 427–446. https://doi.org/10.1016/j.saa.2014.02.160

Refat, M. S.; Al-Azab, F. M.; Al-Maydama, H. M. A.; Amin, R. R.; Jamil, Y. M. S. Synthesis and in vitro microbial evaluation of La(III), Ce(III), Sm(III) and Y(III) metal complexes of vitamin B6 drug. *Spectrochim. Acta A Mol. Biomol. Spectrosc*. **2014b**, *127*, 196–215. https://doi.org/10.1016/j.saa.2014.02.043

Refat, M. S.; Al-Azab, F. M.; Al-Maydama, H. M. A.; Amin, R. R.; Jamil, Y. M. S.; Kobeasy, M. I. Synthesis, spectroscopic and antimicrobial studies of La(III), Ce(III), Sm(III) and Y(III) metformin HCl chelates. *Spectrochim. Acta A Mol. Biomol. Spectrosc*. **2015**, *142*, 392–404. https://doi.org/10.1016/j.saa.2015.01.096

Reiss, A.; Cioteră, N.; Dobrițescu, A.; Rotaru, M.; Carabete, A. C.; Parisi, F.; Gănescu, A.; Dăbuleanu, I.; Spînu, C. I.; Rotaru, P. Bioactive Co(II), Ni(II), and Cu(II) complexes containing a tridentate sulfathiazole-based (ONN) Schiff base. *Molecules.* **2021**, *26* (10), 3062. https://doi.org/10.3390/molecules26103062

Safoura, F. Novel Synthesis of Schiff bases Bearing Glucosamine Moiety. *Res. J. Chem. Sci.* **2014**, *4* (2), 25–28.

Sakhare, D. T.; Chondhekar, T. K.; Shankarwar, S. G.; Shankarwar, A. G. Synthesis, characterization of some transition metal complexes of bidentate Schiff base and their antifungal and antimicrobial studies. *Adv. Appl. Sci. Res.* **2015**, *6* (6), 10–16.

Salawu, O. W.; Wuana, R. A.; Ashimom, J. T. Synthesis, characterization and corrosion inhibition of Co (II), Ni (II), Cu (II), and Zn (II) complexes derived from nicotinic acid hydrazide. In *39th CSN Annual International Conference*. Port Harcourt: Academic Journals; 2018, pp 2–6.

Sarwar, A.; Shamsuddin, M. B.; Lingtang, H. Synthesis, characterization and luminescence studies of metal-diimine complexes. *Mod. Chem. Appl.* **2018**, *6* (3), 1000262. https://doi.org/10.4172/2329-6798.1000262

Savalia, R. V.; Patel, A. P.; Trivedi, P. T.; Gohel, H. R.; Khetani, D. B. Rapid and economic synthesis of Schiff base of salicylaldehyde by microwave irradiation. *Res. J. Chem. Sci.* **2013**, *3* (10), 97–99.

Sharma, P. K.; Sen, A. K.; Dubey, S. N. Synthetic, spectral and thermal studies of cobalt(II), nickel(II), zinc(II) and cadmium(II) complexes with amino acid Schiff bases. *Indian J. Chem.* **1994**, *33* (A), 1031–1033.

Shneine, J. K.; Qassem, D. Z.; Mahmoud, S. S. Synthesis, characterization, and antibacterial activity of some amino acid derivatives. *Int. J. Chemtech Res.* **2017**, *10* (3), 604–612.

Tulu, M. M.; Yimer, A. M. Catalytic Studies on Schiff Base Complexes of Co (II) and Ni (II) using benzoylation of phenol. *Mod. Chem. Appl.* **2018**, *6* (3), 1000260. https://doi.org/10.4172/2329-6798.1000260

Yousef, E.; Radwan, L.; Othman, M. A. Synthesis of Co (II) and Cu (II) complexes with NO and N_2O_2 ligands derived from salicylaldehyde. *Chem. Mater. Res.* **2016**, *8* (7), 82–93.

Eclética Química, vol. 48, n. 2, 2023, 66-82
ISSN: 1678-4618
DOI: 10.26850/1678-4618eqj.v48.2.2023.p66-82